

Torque Sensor based Powertrain Control

Master's Thesis
carried out at **DaimlerChrysler AG**
for **The Division of Vehicular Systems**

by
Fredrik Marciszko

Reg nr: LiTH-ISY-EX-3434-2004

June 2, 2004

Torque Sensor based Powertrain Control

Master's Thesis

carried out for **The Division of Vehicular Systems,
Dept. of Electrical Engineering
at Linköpings universitet**

by **Fredrik Marciszko**

Reg nr: LiTH-ISY-EX-3434-2004

Supervisors: **Dr. Wolfgang Staiger**

Powertrain Control, DaimlerChrysler AG

Anders Fröberg

Division of Vehicular Systems, Dept. of E.E.,
Linköpings universitet

Examiner: **Professor Lars Nielsen**

Division of Vehicular Systems, Dept. of E.E.,
Linköpings universitet

Linköping, June 2, 2004

	Avdelning, Institution Division, Department Vehicular Systems, Dept. of Electrical Engineering 581 83 Linköping	Datum Date June 2, 2004
	Språk Language <input type="checkbox"/> Svenska/Swedish <input checked="" type="checkbox"/> Engelska/English <input type="checkbox"/> _____	Rapporttyp Report category <input type="checkbox"/> Licentiatavhandling <input checked="" type="checkbox"/> Examensarbete <input type="checkbox"/> C-uppsats <input type="checkbox"/> D-uppsats <input type="checkbox"/> Övrig rapport <input type="checkbox"/> _____
URL för elektronisk version http://www.vehicular.isy.liu.se http://www.ep.liu.se/exjobb/isy/2004/3434/		
Titel Momentsensorbaserad drivlinereglering Title Torque Sensor based Powertrain Control		
Författare Fredrik Marciszko Author		
Sammanfattning Abstract <p>The transmission is probably the drivetrain component with the greatest impact on driveability of an automatic transmission equipped vehicle. Since the driver only has an indirect influence on the gear shift timing, except for situations like kick-down accelerations, it is desirable to improve shift quality as perceived by the driver. However, improving shift quality is a problem normally diametrically opposed to minimizing transmission clutch energy dissipation. The latter has a great impact on transmission lifetime, and has to be defined and taken into consideration along with the notion of shift quality. The main focus of this thesis is the modeling of a drivetrain of an automatic transmission vehicle, and the implementation in MatLab/Simulink, including the first to second gear upshift. The resulting plant based on the derived equations is validated using data from a test vehicle equipped with a torque sensor located at the transmission output shaft. The shaft torque is more or less proportional to the driveline jerk, and hence of great interest for control purposes. Control strategies are discussed and a PID controller structure is developed to control the first to second gear upshift, as opposed to the traditional open-loop upshift control. Furthermore, the proposed controller structure uses the transmission output torque and the differential speed of the engaging clutch as inputs, to control the clutch pressure and the engine output torque, respectively. The structure is unsophisticated and transparent compared to other approaches, but shows great theoretical results in terms of improved shift quality and decreased clutch wear.</p>		
Nyckelord Keywords	Drivetrain Modeling, Shift Quality, Clutch Wear, Vehicle Jerk, Automatic Transmission, Torque Sensor, Magnetoelastic, Magnetostrictive	

Abstract

The transmission is probably the drivetrain component with the greatest impact on driveability of an automatic transmission equipped vehicle. Since the driver only has an indirect influence on the gear shift timing, except for situations like kick-down accelerations, it is desirable to improve shift quality as perceived by the driver. However, improving shift quality is a problem normally diametrically opposed to minimizing transmission clutch energy dissipation. The latter has a great impact on transmission lifetime, and has to be defined and taken into consideration along with the notion of shift quality. The main focus of this thesis is the modeling of a drivetrain of an automatic transmission vehicle, and the implementation in MatLab/Simulink, including the first to second gear upshift. The resulting plant based on the derived equations is validated using data from a test vehicle equipped with a torque sensor located at the transmission output shaft. The shaft torque is more or less proportional to the driveline jerk, and hence of great interest for control purposes. Control strategies are discussed and a PID controller structure is developed to control the first to second gear upshift, as opposed to the traditional open-loop upshift control. Furthermore, the proposed controller structure uses the transmission output torque and the differential speed of the engaging clutch as inputs, to control the clutch pressure and the engine output torque, respectively. The structure is unsophisticated and transparent compared to other approaches, but shows great theoretical results in terms of improved shift quality and decreased clutch wear.

Keywords: Drivetrain Modeling, Shift Quality, Clutch Wear, Vehicle Jerk, Automatic Transmission, Torque Sensor, Magnetoelastic, Magnetostrictive

Acknowledgments

Dr. Wolfgang G. Staiger is acknowledged for supporting throughout the thesis work. The author would also like to acknowledge Prof. Dr.-Ing. Pfeiffer, Institute of Applied Mechanics, Munich, Germany, Prof. Dr. H. P. Geering, Institut für Mess- und Regeltechnik, Zurich, Switzerland, Assistant Professor Jonas Fredriksson, Chalmers University of Technology, Gothenburg, Sweden, and Professor Dong-II D. Cho, Seoul National University, Seoul, South Korea, for their prompt answers to literature requests. Not to forget, everyone that provided feedback on this report, including Anders Fröberg with the Division of Vehicular Systems, are greatly acknowledged.

Contents

Abstract	v
Acknowledgments	vi
1 Introduction	1
1.1 Background	1
1.2 Purpose	1
1.3 Method and Outline	1
1.4 The Test Vehicle	2
2 Automatic Transmission Overview	3
2.1 Torque Converter	3
2.2 Planetary Gear Sets	5
2.3 Shift Logic	6
3 Vehicle Modeling	10
3.1 Basic Drive Train Equations	10
3.1.1 Engine	11
3.1.2 Torque Converter	11
3.1.3 Gear Box	11
3.1.4 Drive Shaft	12
3.1.5 Differential	12
3.1.6 Wheels	12
3.2 The Vehicle Model	12
3.2.1 Engine	12
3.2.2 Drive Shaft	13
3.2.3 Vehicle	13
3.3 Gear Shift Modeling	14
3.3.1 First Gear Equations	16
3.3.2 Torque Phase Equations	16
3.3.3 Inertia Phase Equations	17
3.3.4 Second Gear Equations	17
3.4 Model Implementation	18

3.5	Model Results and Verification	19
4	Upshift Control	22
4.1	Shift Quality	23
4.1.1	As Perceived by the Driver	23
4.1.2	Hardware Aspects	23
4.2	Brief Upshift Control Survey	23
4.3	Torque Sensor Based Upshift Control	24
4.3.1	Basic Idea and Presumptions	24
4.3.2	Closed Loop Simulations	26
5	Conclusions	31
6	Further Work	32
	References	33
	Notation	35
A	Torque Sensing	38
A.1	Sensor Principles	39
A.2	Sensor Location	40
A.2.1	Between Engine and Transmission	40
A.2.2	Behind Transmission	41

List of Tables

- 2.1 Chrysler 45RFE Forward Gear Ratios 6
- 4.1 Open and Closed Loop Results, with no Actuator Dynamics 29
- 4.2 Open and Closed Loop Results, Actuator Dynamics and Noise 29

List of Figures

1.1	The Jeep Grand Cherokee	2
2.1	Cut Away View of an Automatic Transmission	4
2.2	Torque Converter Schematics [11]	5
2.3	Constituents of a Planetary Gear Set [3]	6
2.4	Gear Set from the 45RFE Transmission	7
2.5	The 45RFE Planetary Gear Set without the Sun Gear	8
2.6	A Compound Planetary Gear Set [7]	8
2.7	45RFE Transmission Shift Schedule	9
3.1	Schematic Drawing of a Drive Train Model	11
3.2	Pacejka Tire Model Curves [6]	14
3.3	Inertia Model	15
3.4	Signal Flow Chart for the Simulink Model	19
3.5	Modeled Transmission Output Torque	20
3.6	Measured and Filtered Real Torque Signal	21
3.7	Modeled Power Train Speeds During the 1-2 Gear Shift	21
4.1	1-2 Upshift Torque: Output (solid) vs. Desired Ideal (dashed)	22
4.2	Torque Phase Controller Parameter Evaluation	26
4.3	Inertia Phase Controller Parameter Evaluation	27
4.4	Controlled Upshift, no Actuator Dynamics	27
4.5	Vehicle Jerk, Open Loop	28
4.6	Vehicle Jerk, Closed Loop, no Actuator Dynamics	28
4.7	Controlled Upshift with Actuator Dynamics and Noise	30
4.8	Vehicle Jerk, Closed Loop with Actuator Dynamics and Noise	30
A.1	Schematics of the Magnetolestic Sensor [23]	41

Chapter 1

Introduction

1.1 Background

This thesis work is part of a project aimed at making use of a torque sensor implemented in the drive train of an automatic transmission equipped vehicle. The potential benefits from a true torque signal have been extensively discussed and praised, examples of this can be found in [4, 8]. In this particular case the sensor is located at the output shaft of the transmission and hence ideal for monitoring the latter¹. In an early stage of this work it was decided to use the torque signal for feedback control of an upshift. In doing so the upshift feel and the wear on the involved friction elements can be positively affected.

1.2 Purpose

The main purpose with this thesis is to model a one wheel automatic transmission equipped vehicular drive train. The most important aspect of the modeling is to capture the first to second gear upshift dynamics. The idea is to use the derived model for trying out future control strategies for feedback control of the transmission, using the torque signal from the transmission output. Within the scope of this thesis is also the development of a feedback control structure for improving shift quality and decreasing clutch wear.

1.3 Method and Outline

A mathematical representation of the vehicle model is derived and implemented in MatLab/Simulink. Different models are developed for open loop and closed loop control, see Chapter 4. For the first to second gear upshift

¹Different sensor principles and implementation locations are surveyed in Appendix A

considered in this work, two clutches are involved from which one is a wet friction clutch and the other is a sprag-type one-way clutch. Since the vehicle jerk and the clutch energy dissipation are diametrically opposed, e.g. [15, 21], it must be decided how to weight these two aspects. Also, decisions about what to control and to what extent that is possible, are issues addressed in Chapter 4. Because of the nonlinearities of the model, see for example Section 2.1, and simplicity reasons, a PID controller structure is developed and tuned for a specific load case.

1.4 The Test Vehicle

The test vehicle is a Jeep Grand Cherokee Limited, see Figure 1.1, with a 4.7 liter engine. It is equipped with a five speed automatic transmission from Chrysler, namely the 45RFE. During this thesis work, torque data was collected for model verification using a Blue Tooth equipped PDA running an in-house developed software. The test data presented is filtered using a median filter with length 3.



Figure 1.1: The Jeep Grand Cherokee

Chapter 2

Automatic Transmission Overview

The automatic transmission (AT), is a rather complex mechatronic device introduced in the 1930's. However, it was not until later it became a good alternative, continuously growing in popularity, to the traditional manual transmission. Its automated gear shifting makes driving less stressful and hence helps the driver stay attentive. Moreover, the AT features a torque amplification and enables the vehicle to stand still although a gear ratio is selected.

The AT comprises a hydrodynamic torque converter, a number of planetary gear sets, clutches, brake bands, and a hydraulic actuator unit along with the electronic control unit. The latter contains the shift logic, determining when a gear shift should take place. The different gear ratios are realized by combining the different gear sets using the clutches and the break bands.

The input and output speeds are normally measured using inductive sensors. In the Chrysler 45RFE transmission the speeds are measured with a resolution of 30 pulses per revolution on the input side, and 60 on the output side. The power transmitting constituents and the shift logic of an AT are further discussed in the sections below. An AT is schematically depicted in Figure 2.1, the input side facing left.

2.1 Torque Converter

The torque converter (TC), is a hydrodynamic device mechanically separating the engine output shaft and the input shaft of the gear box. It consists of a pump and a turbine, according to Figure 2.2.

The pump is directly connected to the output shaft of the engine, while the turbine is connected to the input shaft of the gearbox. The TC is filled with a hydraulic oil which is the medium transferring the engine torque to the gear box. There is also a stator located between the pump and the turbine essential

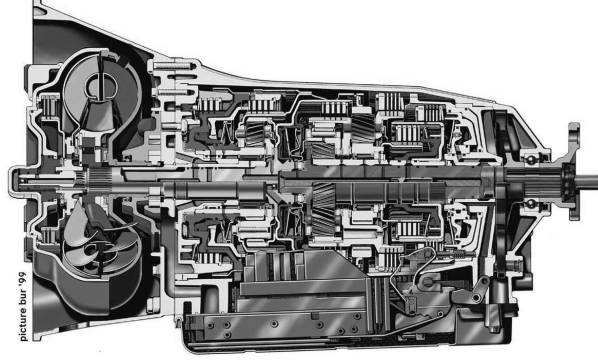


Figure 2.1: Cut Away View of an Automatic Transmission

for the converter function. It works as a driving unit and it helps direct the fluid reducing turbulence. Because of the hydrodynamic coupling there is always a slip in the TC, contributing to the AT's lower efficiency compared to a manual transmission. However, this parasitic loss is normally reduced for higher gears by closing a clutch connecting the pump and turbine when the level of slip is small enough. This clutch is referred to as a lock-up clutch, but is not considered in this work since only the first to second gear upshift is modeled.

The torque transferred by the TC can be approximated with a function of the pump and turbine speeds, according to e.g. [5, 11]. The reaction torque from the pump side of the TC can be calculated as

$$T_p = \left[\frac{\dot{\theta}_p}{f_c \left(\frac{\dot{\theta}_t}{\dot{\theta}_p} \right)} \right]^2 \quad (2.1)$$

and the output turbine torque as

$$T_t = T_p f_t \left(\frac{\dot{\theta}_t}{\dot{\theta}_p} \right) \quad (2.2)$$

where $\dot{\theta}$ denotes angular speed and the indexes p and t represents pump and turbine, respectively. f_c and f_t are look-up tables converting the speed ratio to a capacity factor and a torque ratio.

The look-up tables used in Equations (2.1) and (2.2) reflect the fact that the TC torque amplification is greater at higher speed differences. The speed

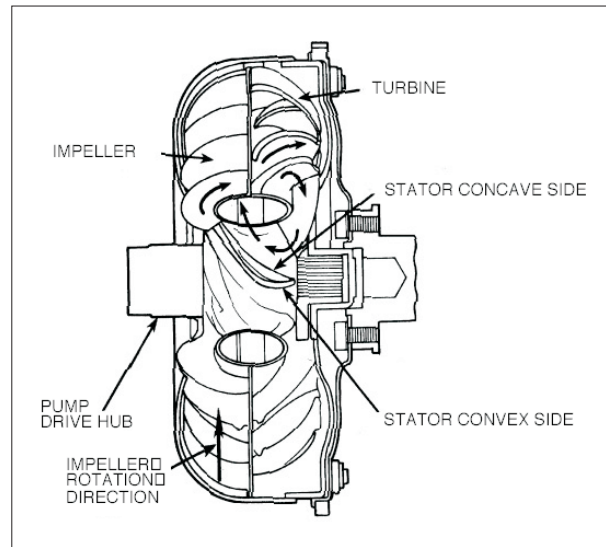


Figure 2.2: Torque Converter Schematics [11]

difference dependability of the torque is the reason an automatic transmission can transfer more torque than a manual, especially at take-off when the speed difference is large. With a gear engaged and engine at idle very little torque is being transferred, enabling the vehicle to keep stationary applying just a little bit of brakes. Refer to [5] for a thorough explanation of the TC and its properties.

2.2 Planetary Gear Sets

The Chrysler 45RFE transmission [9] has three planetary gear sets (PGS), making it possible to realize six different forward gear ratios, see Table 2.1. However, the gear ratio denoted 4* is not supported in the control logic. 2* denotes a gear with a ratio not differing much from the ratios of the 2nd nor the 3rd gear, facilitating a smoother and faster ratio change for kick-down situations.

A PGS basically comprises a carrier with a set of smaller pinion gears, a sun gear, and an internal gear. See Figure 2.3 for an illustration. When a PGS is part of the torque flow path through the transmission, one of the gears is the input, another is prevented from moving, and the third gear is the output gear. By letting different gears represent output and input gears it is possible to create a number of ratios from one single PGS. The actual output PGS of the 45RFE can be seen in Figures 2.4, and 2.5. In addition, Figure 2.4 displays

<i>Gear</i>	<i>Gear Ratio</i>
1 st	3.00
2 nd	1.67
2*	1.50
3 rd	1.00
4 th	0.75
4*	0.67

Table 2.1: Chrysler 45RFE Forward Gear Ratios

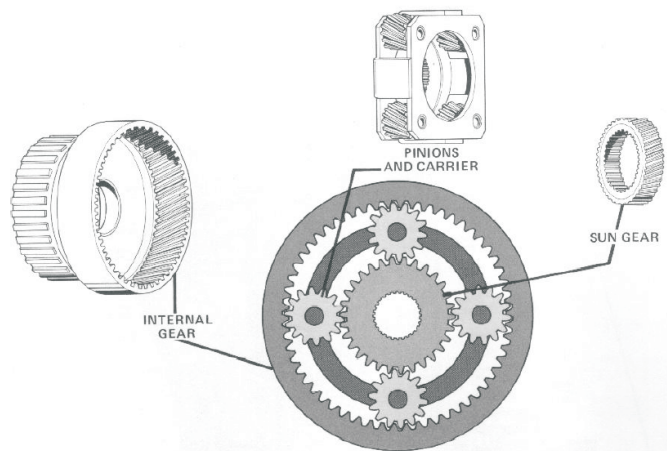


Figure 2.3: Constituents of a Planetary Gear Set [3]

the electroplated copper pattern that is part of the torque sensor discussed in Appendix A.

Although the 45RFE transmission contains three planetary gear sets only two of them are involved in the first to second gear upshift. Figure 2.6 demonstrates the interconnection between the modeled equivalent compound PGS and other parts of the power train.

2.3 Shift Logic

The main function of the shift logic implemented in the transmission control unit (TCU), is to use the throttle angle and the transmission output speed to determine when to order an up or downshift. There is a number of shift patterns used in the 45RFE depending on the transmission temperature. This is



Figure 2.4: Gear Set from the 45RFE Transmission

to improve shift feel, especially at very cold temperatures. The hot/normal shift pattern for the 45RFE transmission partly implemented in the Simulink model is illustrated in Figure 2.7. When a shift command is given, the involved hydraulic clutch actuators are being pressurized, for the upshift to take place.

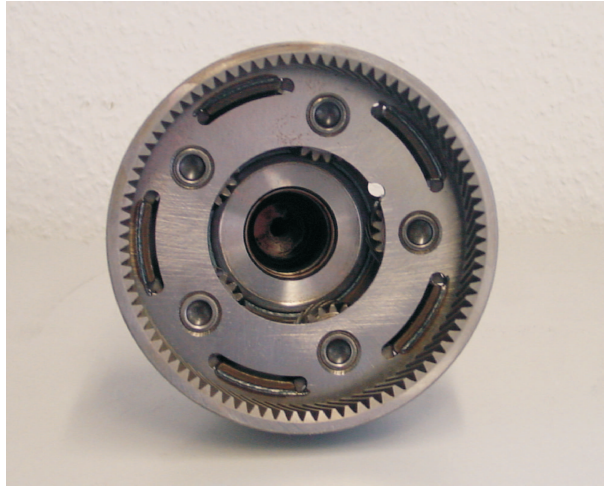


Figure 2.5: The 45RFE Planetary Gear Set without the Sun Gear

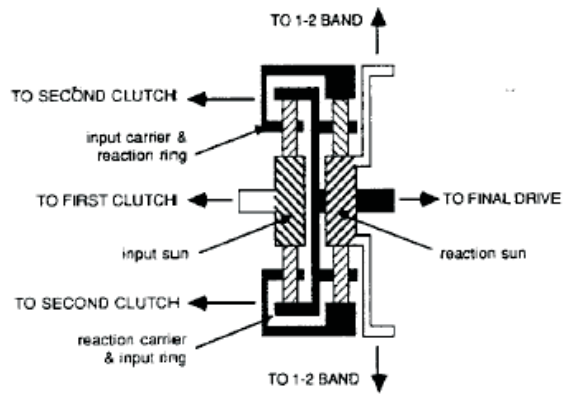


Figure 2.6: A Compound Planetary Gear Set [7]

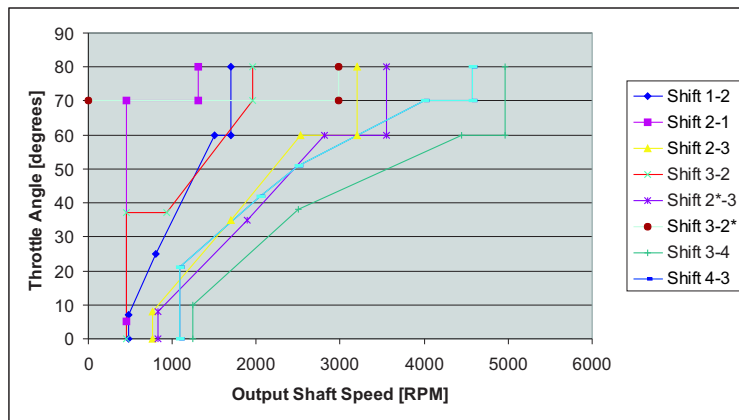


Figure 2.7: 45RFE Transmission Shift Schedule

Chapter 3

Vehicle Modeling

The model derived in this thesis is partly based on a one-wheel vehicle model readily available at the Powertrain Control department with Daimler Chrysler. This model was rebuilt and improved to specifically serve the first to second gear upshift simulation purpose. In order to implement the vehicle model for simulation in MatLab/Simulink [18], it has to be represented in a mathematical way. In this chapter the drive train equations are derived from a lumped inertia model, using Newton's Second Law of Motion:

$$I\ddot{\theta} = T \quad (3.1)$$

where the capital letter I denotes the body inertia, $\ddot{\theta}$ the angular acceleration of the body, and T the resulting torque. Pettersson outlines similar modeling in [20]. A simplified linear wheel slip model and a lumped drive line elasticity is implemented to describe some of the most important driveline dynamics. Further details are added to the model dynamics as the upshift of the automatic transmission is introduced.

3.1 Basic Drive Train Equations

The equations that follow are more or less general equations for representing the vehicle model, together with given look up tables. Figure 3.1 describes the basic drive train model and its properties. As the figure indicates there are yet no elasticities considered. Please refer to the Notation chapter for variable and parameter names.

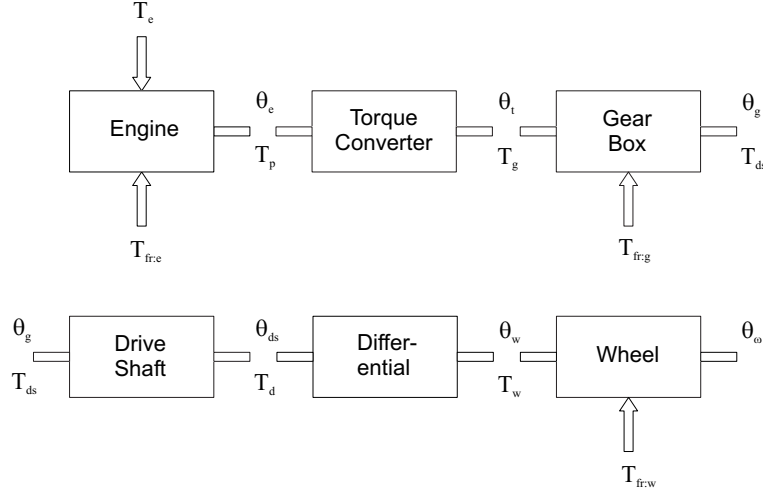


Figure 3.1: Schematic Drawing of a Drive Train Model

3.1.1 Engine

The engine's main constituent is a look up table with engine speed and throttle angle as inputs and engine torque as output.

$$I_e \ddot{\theta}_e = T_e - T_{fr:e} - T_p \quad (3.2)$$

3.1.2 Torque Converter

T_p and T_t are calculated as functions of the pump and turbine speed difference as described in Section 2.1

$$I_p \ddot{\theta}_p = T_e - T_p \quad (3.3)$$

$$\theta_p = \theta_e \quad (3.4)$$

$$I_t \ddot{\theta}_t = T_t - T_g \quad (3.5)$$

3.1.3 Gear Box

The gear box inertia I_g is dependent on the gear ratio i associated with the current gear.

$$I_g(i) \ddot{\theta}_g = i T_g - T_{fr:g} - T_{ds} \quad (3.6)$$

$$\theta_g i = \theta_t \quad (3.7)$$

Equation (3.6) presumes an simplified gear box model with the gear ratio at the input side and the inertia lumped at the output.

3.1.4 Drive Shaft

$$I_{ds}\ddot{\theta}_{ds} = T_{ds} - T_d \quad (3.8)$$

$$\theta_{ds} = \theta_g \quad (3.9)$$

3.1.5 Differential

The gear ratio of the differential is represented by i_{diff} , and η denotes the efficiency of the differential.

$$T_d i_{diff} \eta = T_w \quad (3.10)$$

$$\theta_w i_{diff} = \theta_{ds} \quad (3.11)$$

3.1.6 Wheels

$$I_w \ddot{\theta}_w = T_w - r_w F_w - T_{fr:w} - T_{break} \quad (3.12)$$

$$F_w = m\dot{v} + F_{drag} \quad (3.13)$$

F_{drag} is a sum of air drag, rolling resistance, and the gravitational component associated with road grade. These are calculated from already available look-up tables implemented in the model. See for example [20] for more details on this. The notations r_w , m , and v , is the wheel radius, the vehicle mass and the vehicle speed, respectively.

3.2 The Vehicle Model

The equations presented in Section 3.1 are combined and rewritten to form the outputs from the different Simulink blocks. Also, a detailed upshift of the automatic transmission as well as a lumped drive line elasticity and a linear wheel slip model is discussed and implemented. This is necessary in order to fully describe the vehicle behavior experienced by the driver [17]. The transmission mechanical dynamics is dealt with separately and replaces the above presented gear box block. Additionally, functionality like an engine idle speed controller, is also implemented but not discussed here.

3.2.1 Engine

Combining equations (3.2), (3.3), and (3.4) yields the equation:

$$\ddot{\theta}_p = \frac{T_e - T_{fr:e} - T_p}{I_e + I_p} \quad (3.14)$$

which is valid when the lock-up clutch is open.

3.2.2 Drive Shaft

The drive shaft elasticity is implemented according to [20], introducing two constants, k and c , representing the shaft stiffness and the shaft damping, respectively. The equation for the drive shaft then becomes:

$$T_d = T_{ds} = k(\theta_g - \theta_{ds}) + c(\dot{\theta}_g - \dot{\theta}_{ds}) \quad (3.15)$$

Equation (3.15) replaces the above presented equations (3.8) and (3.9). This drive shaft model does not include the shaft inertia. It is instead evenly distributed to the connecting components.

3.2.3 Vehicle

The wheel acceleration is given by manipulating equations (3.12), (3.13), and (3.10). Neglecting the wheel friction the result turns out as follows:

$$\ddot{\theta}_w = \frac{T_w - r_w F_w - T_{break}}{I_w + mr_w^2} \quad (3.16)$$

Wheel Slip

At moderate wheel slip rates the force acting on the tire can be approximated with a linear function, as opposed to implementing the complete Pacejka formula [19]. Therefore a less complicated linear slip model is introduced assuming the wheel slip proportional to the wheel force F_w . An example of Pacejka tire model curves can be seen in Figure 3.2, indicating the linear properties at lower slip rates. The slip force calculation was chosen according to:

$$F_s = F_w = \mu smg \cos \beta \quad (3.17)$$

where μ is a friction constant, s the wheel slip, m the vehicle mass, g the gravitational constant, and β the road gradient. To calculate the wheel slip s , two different equations can be used. Those are:

$$s = \frac{\dot{\theta}_w r_w - v}{\dot{\theta}_w r_w}, s \geq 0 \quad (3.18)$$

and

$$s = \frac{v - \dot{\theta}_w r_w}{v}, s \leq 0 \quad (3.19)$$

Introducing the wheel slip, and hence separating the calculations of wheel acceleration from vehicle acceleration, yields:

$$\ddot{\theta}_w = \frac{T_w - r_w F_w - T_{break}}{I_w + 0.5 I_{ds} i_{diff}^2} \quad (3.20)$$

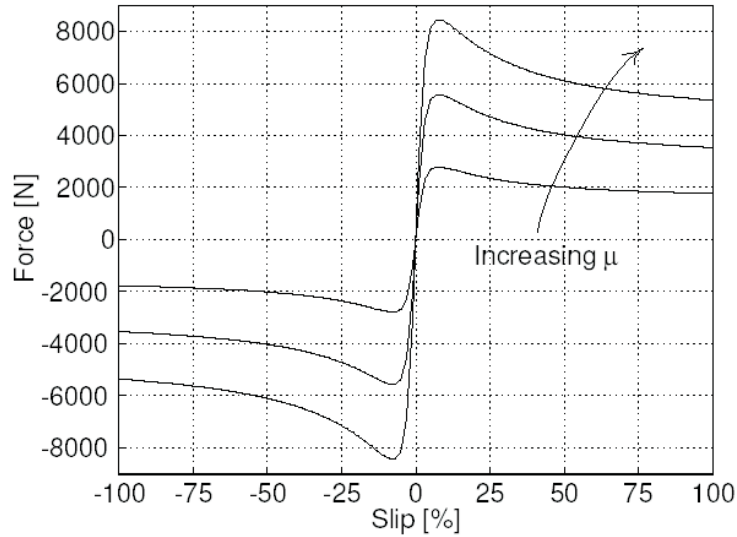


Figure 3.2: Pacejka Tire Model Curves [6]

and

$$\dot{v} = \frac{F_w - F_{drag}}{m} \quad (3.21)$$

In Equation (3.20) half of the drive shaft inertia has been assigned to the wheels, and the other half is incorporated in the gear box output inertia, see Section 3.3. Equations (3.20) and (3.21) along with Equations (3.17), (3.18), and (3.19), replace Equation (3.16) in the implementation.

3.3 Gear Shift Modeling

In reality lower gear upshifts excite the most oscillations and drive line jerk, e.g. [17]. Because of that and to limit the scope of this thesis, the first to second gear upshift is discussed exclusively. To illustrate the conditions and problems associated with this modeling, a lumped inertia model is used, see Figure 3.3. The components of the inertia model used for describing the upshift can be identified in Figure 2.6. As depicted in the figure there are two clutches involved in the upshift, and that is why the upshift is described by two dynamic processes, or transitional phases, e.g. [3, 17]. Clutch number one is a one-way clutch and number two is a wet clutch. With one-way is meant that it can only transmit torque in one direction, it has a sprag that allows the clutch to free-wheel when subjected to “negative” torque [9, 22]. This discussion leads to the following four separate consecutive modes:

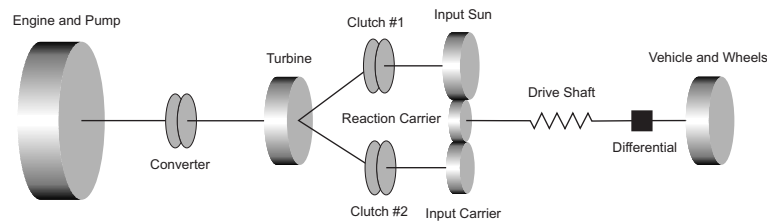


Figure 3.3: Inertia Model

First Gear The transmission stays in first gear as long as the constraints for that are fulfilled, i.e. the current combination of transmission output speed and throttle angle does not imply an upshift. Clutch number two is open and hence not included in the torque flow. Therefore the one-way clutch is automatically transmitting the turbine torque alone. The gear ratio is determined by the input sun and the reaction carrier gears.

Torque Phase (TP) As soon as the shift logic has ordered an upshift the second clutch starts closing and immediately transmits some torque. At that instant, the onset of the torque phase, the transmission output torque starts dropping. This is inevitable since some of the turbine torque is re-routed via the oncoming clutch. The torque transmitted by the first clutch is decreasing throughout this phase, up to the point when it starts free-wheeling. When that happens the next phase begins. The duration of the torque phase is normally $150 - 200ms$.

Inertia Phase (IP) Now the second clutch is transmitting all turbine torque alone, but is yet not fully closed. The gear ratio is indeterminate, but is assuming the second gear ratio as the clutch continues to engage. This phase is characterized by a sudden increase in transmission output torque caused by the gear ratio change and the decelerating inertia of mainly the engine. This torque overshoot eventually goes down to the second gear output torque level, leaving a hump in the torque history. The inertia phase is also called the speed phase, referring to the speeds of the clutch coming to a match. The duration of this phase is approximately $500ms$.

Second Gear The transmission is in second gear as soon as the second clutch is considered closed. The new gear ratio is determined by the input carrier and the reaction carrier gears. There are constraints to be fulfilled to stay in second gear, but they are not considered here since only the upshift process is of interest.

The following shift modeling is outlined in [3, 22], according to [7] with the discussion above in mind.

3.3.1 First Gear Equations

The state equation and the kinematic constraints of interest for determining the gear box outputs in first gear can be written in the following way:

$$I_{t1}\ddot{\theta}_t = T_t - \frac{T_{ds}}{i_1} \quad (3.22)$$

$$\dot{\theta}_{cr} = \frac{\dot{\theta}_t}{i_1} \quad (3.23)$$

$$\dot{\theta}_{ci} = \dot{\theta}_t \frac{i_2}{i_1} \quad (3.24)$$

$$\dot{\theta}_{si} = \dot{\theta}_t \quad (3.25)$$

$$\dot{\theta}_{sr} = 0 \quad (3.26)$$

where

$$I_{t1} = I_t + I_{si} + I_{ci} \left(\frac{i_2}{i_1} \right)^2 + \frac{I_{cr}}{i_1^2} \quad (3.27)$$

3.3.2 Torque Phase Equations

When the second, or new, clutch starts transmitting torque, the state equation becomes:

$$I_{t1}\ddot{\theta}_t = T_t - \frac{T_{ds}}{i_1} - T_{c2} \left(1 - \frac{i_2}{i_1} \right) \quad (3.28)$$

However, the kinematic constraints remain the same according to Equations (3.23), (3.24), (3.25), and (3.26). Also, I_{t1} is still determined according to (3.27).

The torque transferred by the engaging clutch can be calculated in the following way:

$$T_{c2} = AR_{c2}\mu_{c2}P_{c2}\text{sgn}(c2_{slip}) \quad (3.29)$$

where AR_{c2} and P_{c2} is the clutch area and the pressure applied on the clutch, respectively. The equation used for calculating the friction coefficient μ_{c2} is:

$$\mu_{c2} = \mu_1 + \mu_2 |c2_{slip}| \quad (3.30)$$

where

$$c2_{slip} = \dot{\theta}_t - \dot{\theta}_{ci} \quad (3.31)$$

3.3.3 Inertia Phase Equations

The inertia phase starts as soon as the first clutch sprag reaction torque is equal to or less than zero. During this phase, the first clutch is not transmitting any torque and the second one is still slipping, therefore two state-equations are needed to describe the dynamics:

$$I_{cr12}\ddot{\theta}_{cr} = T_{c2}i_2 - T_{ds} \quad (3.32)$$

and

$$I_t\ddot{\theta}_t = T_t - T_{c2} \quad (3.33)$$

The kinematic constraints become:

$$\dot{\theta}_{ci} = \dot{\theta}_{cr}i_2 \quad (3.34)$$

$$\dot{\theta}_{si} = \dot{\theta}_{cr}i_1 \quad (3.35)$$

$$\dot{\theta}_{sr} = 0 \quad (3.36)$$

The first clutch sprag reaction torque is:

$$T_{Rsp1} = \frac{T_{ds}}{i_1} - T_{c2}\frac{i_2}{i_1} + I_{si12}\ddot{\theta}_{si} \quad (3.37)$$

3.3.4 Second Gear Equations

When the second gear clutch has stopped slipping and is locked, the inertia phase is considered completed. To determine whether the clutch is locked or not, two conditions have to be fulfilled:

- The clutch capacity \geq than the clutch reaction torques
- The clutch slip = 0

The reaction torques acting across the clutch are:

$$T_{Rc2up} = T_t - I_t\ddot{\theta}_t \quad (3.38)$$

and

$$T_{Rc2down} = I_{ci12}i_2\ddot{\theta}_{cr} + \frac{T_d}{i_2} \quad (3.39)$$

Equation (3.31) yields the clutch slip.

The second gear equations are similar to the equations describing the state and kinematic constraints associated with first gear:

$$I_{t2}\ddot{\theta}_t = T_t - \frac{T_{ds}}{i_2} \quad (3.40)$$

$$\dot{\theta}_{cr} = \frac{\dot{\theta}_t}{i_2} \quad (3.41)$$

$$\dot{\theta}_{ci} = \dot{\theta}_t \quad (3.42)$$

$$\dot{\theta}_{si} = \dot{\theta}_t \frac{i_1}{i_2} \quad (3.43)$$

$$\dot{\theta}_{sr} = 0 \quad (3.44)$$

where

$$I_{t2} = I_t + I_{ci} + I_{si} \left(\frac{i_1}{i_2} \right)^2 + \frac{I_{cr}}{i_2^2} \quad (3.45)$$

3.4 Model Implementation

The vehicle model and the transmission model is implemented in MatLab/Simulink. Figure 3.4 indicates the resulting Simulink model signal flow. The automatic transmission plant model has received special attention, and it is divided into several subsystems:

- The shift logic
- The actuator model
- The clutch model
- The reaction torque calculations
- The state computations

The shift logic is implemented using Simulink/Stateflow and outputs the gear shift trigger signal to the actuator model. When a gear shift is demanded, the open loop actuator applies a predefined pressure profile on the second clutch. The used pressure profile is extracted from empirical data and presented in [7]:

$$P_{c2} = P_0 \left[1 - e^{-t/\tau} \right] \quad (3.46)$$

where P_0 is the maximum pressure and τ is a time constant. This is a simplification justified by the complexity of a more vastly detailed model of the hydraulic system. The clutch model on its part uses Equation (3.29) to calculate the transferred torque. The reaction torque calculations (3.37), (3.38), and (3.39), are implemented separately and the results are fed to the clutch model and a state machine determining the timing of the gear shift phases. The state machine then activates the differential equations accordingly.

The majority of the parameter values used in the Simulink model are sound and extracted from DaimlerChrysler documentation. Complementary, not readily available data, have been substituted with values from e.g. [3], and the General Motors Hydramatic 440 Automatic Transmission.

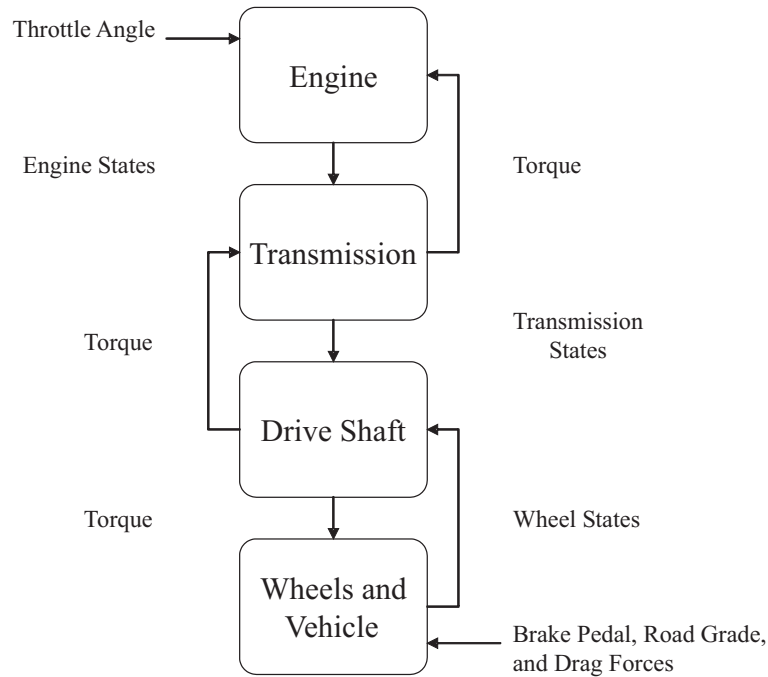


Figure 3.4: Signal Flow Chart for the Simulink Model

3.5 Model Results and Verification

Simulations have been run with 75 per cent open throttle from stationary on a flat surface without braking. Comparing simulation results from the implemented model to [13] shows good overall agreement. The implemented drive shaft torsion and the wheel slip shows good behaviour. The modeled transmission output torque for the first to second gear upshift is depicted in Figure 3.5. The data does not only show details like the typical initial 200 ms hesitation [7], but also good agreement throughout the shift process. Figure 3.6 shows data from a real torque signal collected under similar conditions as those of the simulation in Figure 3.5. The graphs indicate similar behavior, although the data is from one single test run only. The accelerator pedal angle has not been identified, which prevents further conclusions from being drawn. Focusing on the upshift however, it can be concluded that the model agrees well with the measured data. Above all the duration of the upshift shows to be dependent on the applied pressure profile, hence tuning might improve the result further. Moreover, the different powertrain speeds shown in Figure 3.7 agree with the expected behavior, keeping Figure 3.3 in mind.

The verification of the model suggests it as being sound and good for

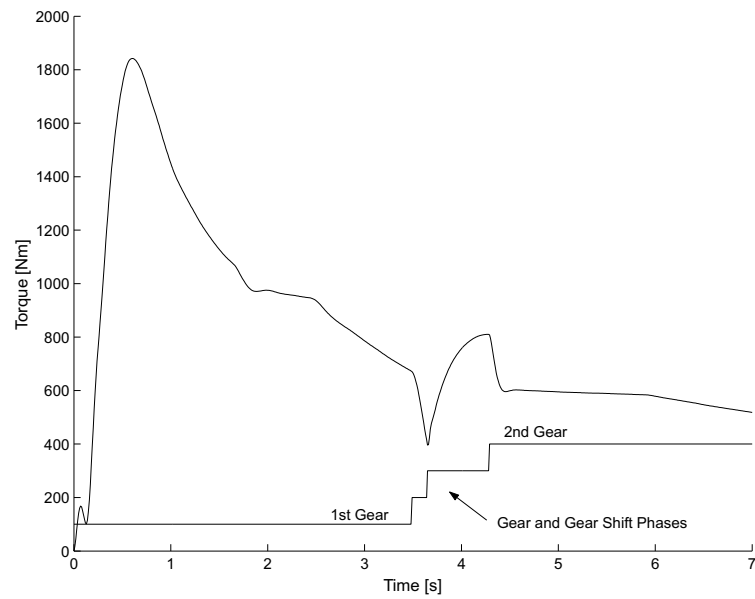


Figure 3.5: Modeled Transmission Output Torque

simulation of the first to second gear upshift of the 45RFE transmission. The transmission is described detailed enough in order to use it in a closed-loop control arrangement under conditions similar to those of the simulation.

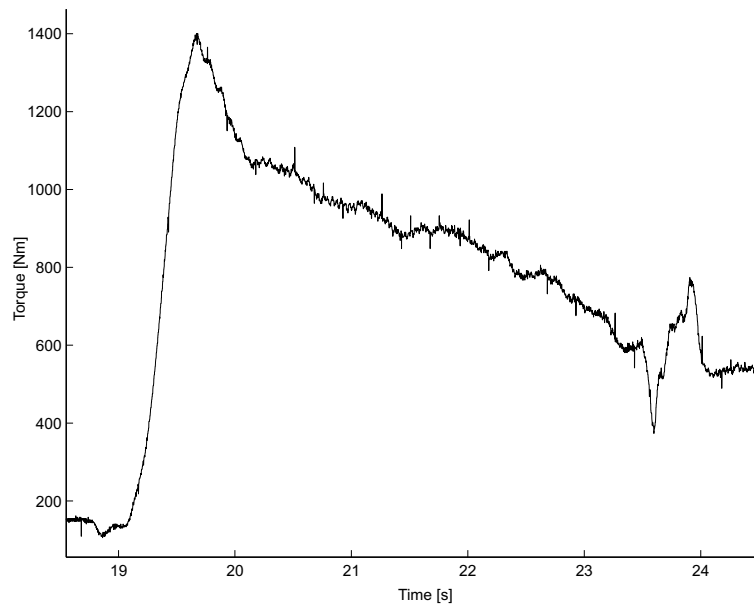


Figure 3.6: Measured and Filtered Real Torque Signal

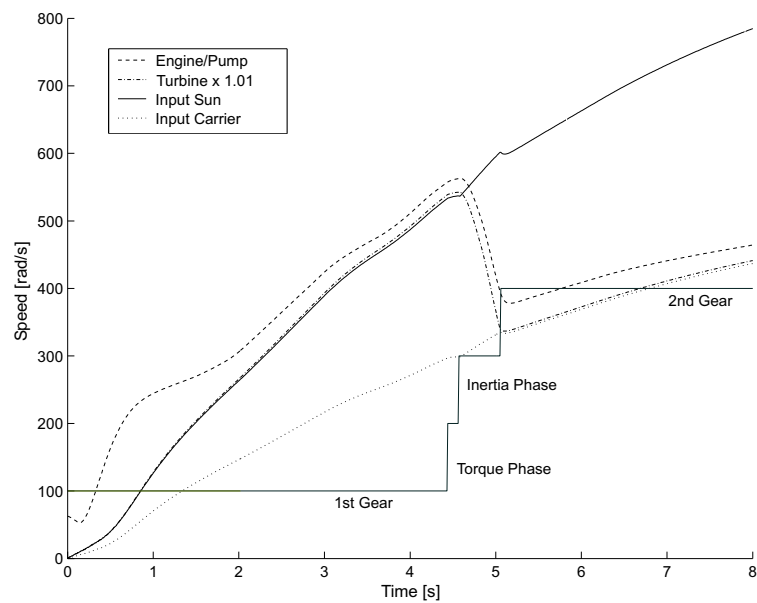


Figure 3.7: Modeled Power Train Speeds During the 1-2 Gear Shift

Chapter 4

Upshift Control

This chapter is discussing upshift control and proposes a strategy for improving shift feel and reducing clutch wear using the developed Simulink model. Shift feel can be improved by smoothing out the transmission output torque during the upshift. See Figure 4.1 for a comparison between the open loop output torque versus the desired ideal output torque during the first to second gear upshift. However, the physical constraints that are present hinders a perfect transition between the two output torque levels for first and second gear. As mentioned in Section 3.3, a certain drop has to be allowed for the upshift to complete. The torque overshoot on the other hand, can be reduced substantially, resulting in improved shift quality.

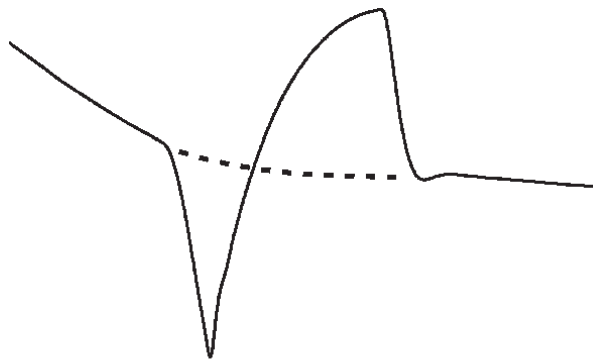


Figure 4.1: 1-2 Upshift Torque: Output (solid) vs. Desired Ideal (dashed)

4.1 Shift Quality

The notion of shift quality can be very subjective and difficult to measure for comparisons unless it is mathematically defined. There are mainly two aspects of shift quality to consider and the following sections will elucidate their signification.

4.1.1 As Perceived by the Driver

An upshift perceived as pleasant by one driver may, or may not, be considered as good by someone else. Since the vehicle jerk can be defined as the time derivative of the vehicle acceleration, \dot{a} , the following equation can be used to measure the jerk for a finite time interval $t - t_0$:

$$C = \int_{t_0}^t \dot{a}^2 dt \quad (4.1)$$

Another criterion possible to use is the integral of the deviation of the measured vehicle acceleration from a predefined desired acceleration profile. That is however not as intuitive to use, since an acceleration profile has to be chosen. Shift duration time is more natural to consider, because it is directly influencing the driver experience and the drivability of the vehicle. From most drivers' point of view the upshift event should occur preferably unnoticed, taking as short a time as possible, to prevent extended output torque discontinuity.

4.1.2 Hardware Aspects

The hardware related issues of shift quality are indirectly related to the driver's perception of the upshift. With extended shift time the wear on the friction elements in the transmission is normally increased, which in turn means shortened transmission life time. The clutch wear can be evaluated using the following expression for the dissipated clutch energy:

$$Q = \int_{t_0}^t \Delta\dot{\phi} T dt \quad (4.2)$$

In this thesis $\Delta\dot{\phi}$ is equal to $c2_{slip}$ in Equation (3.31), and T is the torque transferred by the clutch. At a constant level of transferred torque, Equation (4.2) comes down to a problem of minimizing shift time. However, the transferred torque is approximated with Equation (3.29), and is not constant.

4.2 Brief Upshift Control Survey

There are several ways to control and improve an upshift. The ones surveyed below are probably a mere few of them all, but they should give some per-

spective to the method used in this work.

The most common is to predefine a desired transmission output speed and use that for controlling the clutch pressure, using for instance Lyapunov convergence theory. Absmeier applied so called Sliding Control to the transmission model developed in [3]. The simulations without actuator dynamics show great improvements for the 1-2 gear upshift when it comes to vehicle peak-to-peak acceleration and jerk. Among the pros and cons are improved shift feel using a relatively simple method but to the cost of shift duration, and the method does not consider clutch wear.

A method developed in [14] uses an estimated torque signal and a pre-defined desired torque output, for controlling an electronic throttle to reduce the inertia phase torque overshoot¹. The test set-up includes a physical drive train, and tests show a 30 per cent inertia phase output torque peak-to-peak reduction. The main drawback is the clutch wear is not explicitly taken into consideration.

In for instance [15, 21] optimal control is applied to a model similar to the one presented in this thesis. That leads to a non-linear optimization problem, that has to be solved using cost functions similar to those of Equations (4.1) and (4.2). This is a rather cumbersome way to go and it entails the discretization of the model and solving a minimization problem by means of a sequential quadratic programming algorithm. In [15] the output is a map of pressure and engine torque reduction constants for a specific load case. This method shows very good results using the deviation from a desired acceleration profile and the shift time as cost functions. It appears no actuator dynamics have been considered, and this method can not be seen as being very transparent.

4.3 Torque Sensor Based Upshift Control

The paramount purpose of this thesis is to make use of the torque sensor located at the transmission output shaft. The transmission output torque is a function of the output shaft acceleration according to Equation (3.1), and hence more or less directly proportional to the vehicle acceleration. Because the sensor measures the output torque, it appears ideal to use the sensor signal for improving shift quality by means of closed-loop control.

4.3.1 Basic Idea and Presumptions

The idea is to first create a suitable torque reference signal for controlling the transmission output torque during the upshift. The upshift phases are treated separately, and a reference signal is created for them individually. That is justified by the fact mentioned above, that the output torque has to drop for

¹See for instance Figure 3.6

the upshift to take place. Keeping Figure 3.5 in mind, a downward sloping ramp-shaped reference signal with a slope not extending the torque phase duration too much, should be considered. To reduce the torque overshoot during the inertia phase a reference ramp is created in a similar manner. The inertia phase reference ramp is initiated at the onset of the second phase and its start value is set to the same as of the measured torque at this point, to avoid abrupt changes in the control signal. The slope of the inertia reference signal should be designed so it controls the output torque to the level of the second gear. Section 4.3.2 describes more in detail how the reference signals are created and implemented.

The controller structure comprises a number of PID controllers. There is one pressure controller assigned for each phase of the upshift, and another two for reducing the engine output torque during the inertia phase. If T_{ds} is the measured drive shaft output torque and $T_{des:ds}$ is the reference torque, the error fed to the pressure controller structure can be written

$$e_{pressure} = T_{des:ds} - T_{ds} \quad (4.3)$$

The error signal used by the engine controllers is created using the speed difference of the turbine and the input carrier

$$e_{engine} = w_t - w_{ci} + \delta \quad (4.4)$$

δ in Equation (4.4) compensates for the engine dynamics, both the mechanical originating from the throttle, and the remaining from the intake manifold pressure buildup. The offset is for the throttle control to stop controlling in time, just before the upshift is completed, so the throttle will have time to return to its position of the instant the upshift started. The combined dynamics of the mechanical throttle and torque buildup is modeled as a first order transfer function followed by a transport delay. A total delay of about $180ms$ is accounted for in the model. In addition to controlling the throttle for reducing the engine output torque, one of the controllers is assigned to retard spark advance, promoting virtually instantaneous torque reduction. Hence $\delta = 0$ in this case. It is theoretically possible to achieve an approximate 30 per cent reduction without violating the physical constraints, e.g. temperature and combustion stability [16].

The actuator dynamics is modeled as a first order transfer function [3, 17]

$$P_{actual:c2} = \frac{P_{command:c2}}{\tau s + 1} \quad (4.5)$$

where $P_{actual:c2}$ is the actual pressure exerted by the actuator on the clutch, and $P_{command:c2}$ is the commanded pressure. Furthermore, the time constant is chosen according to

$$\tau = \begin{cases} 0, & \text{No Actuator Dynamics Considered} \\ 0.45, & \text{Actuator Dynamics Considered} \end{cases} \quad (4.6)$$

depending on what kind of closed loop simulation is run.

4.3.2 Closed Loop Simulations

The hardest part of creating the controller is to determine the controller gain and the slope of the reference signals. Vehicle jerk, Equation (4.1), clutch wear, Equation (4.2), and shift time has to be considered. A script was created to run a number of consecutive simulations. The script changes parameters for every run and collects the relevant data. This data given, decisions can be made about how to choose the controller parameters.

Starting with the torque phase, Figure 4.2 clearly shows the relationship between the slope value and dissipated energy. The steeper the slope, the more the jerk, but the less is the dissipated energy. As the figure suggests, decreasing the proportional gain will reduce vehicle jerk but increase clutch wear. Also, a steeper slope will result in shorter shift time and less dissipated energy, but jerk will be increased.

A similar evaluation of the inertia phase yields the same relationships between the controller parameters, see Figure 4.3. Parameters were designed for a model with pressure dynamics implemented, and for one without.

The engine torque reduction parameters are set to utilize the torque reduction possibilities to their fullest extent.

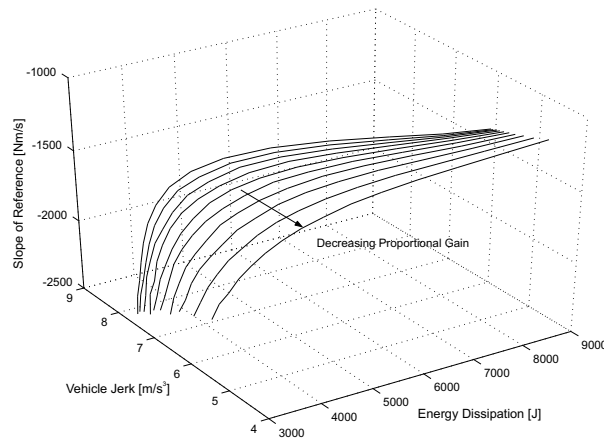


Figure 4.2: Torque Phase Controller Parameter Evaluation

No Actuator Dynamics

Assuming the clutch actuator pressure can be changed instantaneously, i.e. $\tau = 0$ in Equation (4.5), very good results is achieved. Compare Figure 3.5 to Figure 4.4. The latter shows the upshift torque and the reference signals. A pronounced reduction of the torque fluctuation can be seen, without having prolonged the shift time. Vehicle jerk has also been improved, comparing

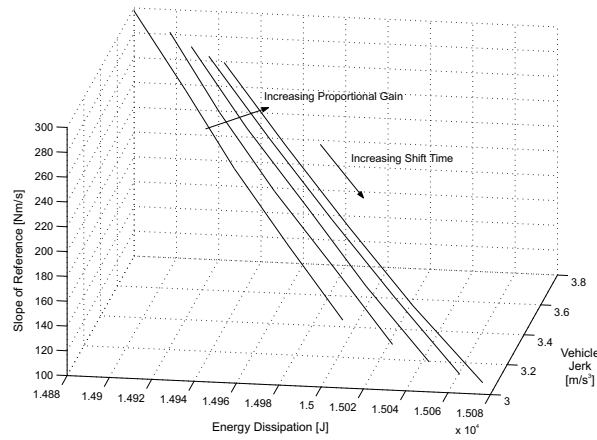


Figure 4.3: Inertia Phase Controller Parameter Evaluation

Figures 4.5 and 4.6 shows a substantial improvement. See Table 4.1 for a

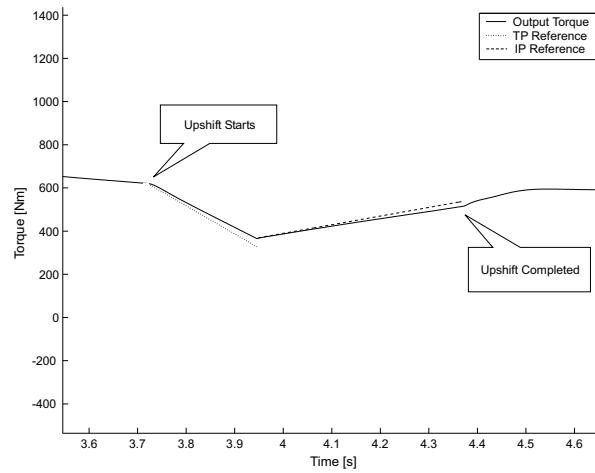


Figure 4.4: Controlled Upshift, no Actuator Dynamics

comparison of the results between the open loop upshift and the simulation without actuator dynamics. The data presented in Table 4.1 indicate a great reduction of vehicle jerk during most of all the last phase of the upshift. The first phase of the shift is also improved, to some cost of dissipated energy. However, both jerk and clutch wear are overall substantially reduced. The

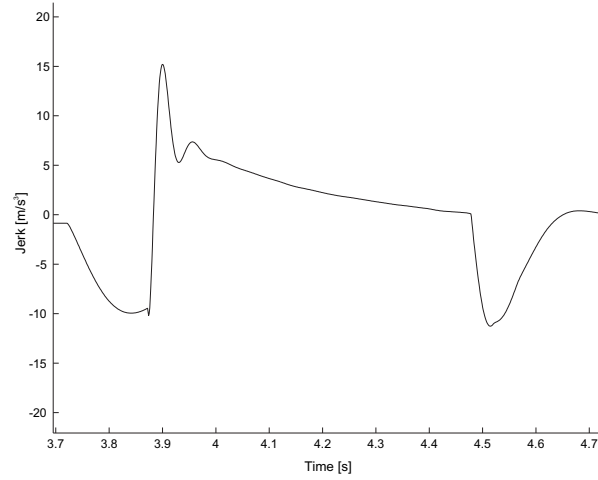


Figure 4.5: Vehicle Jerk, Open Loop

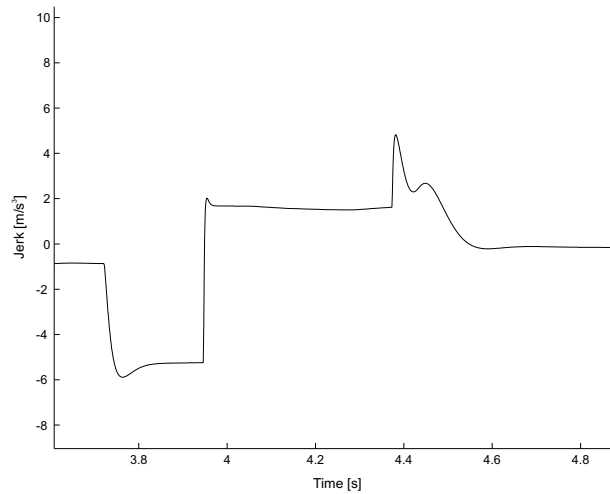


Figure 4.6: Vehicle Jerk, Closed Loop, no Actuator Dynamics

simulations show an approximate 60% jerk reduction and a 40% reduction in clutch wear. Better results are most probably possible to achieve by further tuning, and the results in Table 4.1 are only to be seen as an indication of what results can be expected. Moreover, weighting the two minimizing criteria of jerk and dissipated energy differently would facilitate reaching other results.

	Shift Phase	Open Loop	Closed Loop No Act. Dyn.	Improvement
Vehicle Jerk [m/s^3]	TP	8.75	6.21	29 %
	IP	10.6	1.10	90 %
	TP+IP	19.4	7.31	62 %
Energy Dissipation [$J \cdot 10^4$]	TP	0.457	0.634	-39 %
	IP	2.97	1.51	49 %
	TP+IP	3.43	2.14	38 %

Table 4.1: Open and Closed Loop Results, with no Actuator Dynamics

With Actuator Dynamics

Setting $\tau = 0.45$ in Equation (4.5) introduces a first order pressure model. Under this new condition the clutch pressure is controlled via a first-order lag, resulting in not as good results as previously presented. In addition to the actuator dynamics, band-limited white noise was added to the torque signal used by the controller, to emulate the real world conditions better. To cope with the problems this causes at the creation of the start value of the reference signal, a sliding average filter using the five last samples of the torque signal was implemented. Figure 4.7 shows a typical upshift under these conditions. The vehicle jerk is illustrated in Figure 4.8, and typical data is presented in Table 4.2. The most noticeable difference is the degraded vehicle jerk performance in the inertia phase, assigned to the introduction of the pressure dynamics.

	Shift Phase	Open Loop	Closed Loop Act. Dyn.	Improvement
Vehicle Jerk [m/s^3]	TP	8.75	6.01	31 %
	IP	10.6	4.27	60 %
	TP+IP	19.4	10.3	50 %
Energy Dissipation [$J \cdot 10^4$]	TP	0.457	0.640	-40 %
	IP	2.97	1.52	49 %
	TP+IP	3.43	2.16	37 %

Table 4.2: Open and Closed Loop Results, Actuator Dynamics and Noise

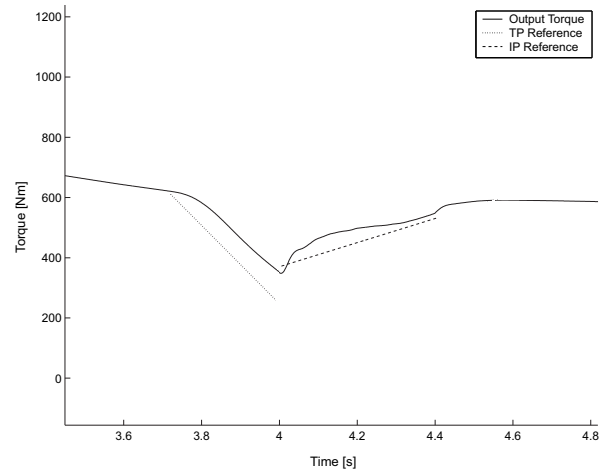


Figure 4.7: Controlled Upshift with Actuator Dynamics and Noise

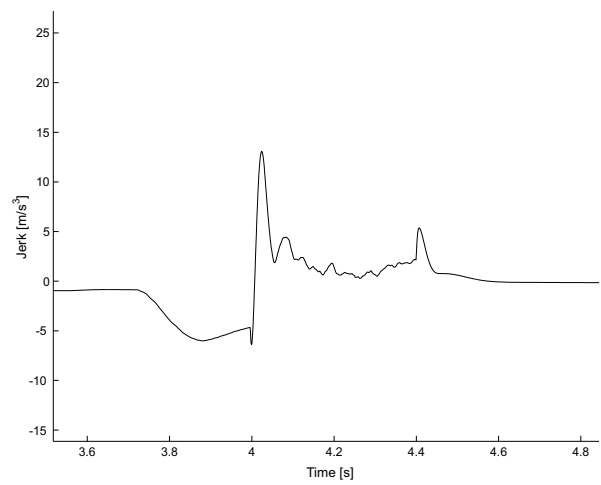


Figure 4.8: Vehicle Jerk, Closed Loop with Actuator Dynamics and Noise

Chapter 5

Conclusions

The drivetrain was successfully modeled and the simulation data verifies it as correct. Summing up the closed loop results concludes a good overall performance of the control strategy using the torque sensor for feed-back control. The results presented in Table 4.1 are specially good, showing a vehicle jerk and clutch wear reduction of **62%** and **38%**, respectively. The jerk reduction in the inertia phase is particularly noticeable with its **90%**, obviously accounting for the largest part of the overall improvement. Introducing the actuator dynamics, the results are deteriorated but can still be seen as satisfactory. The corresponding data in Table 4.2 is a vehicle jerk reduction of **50%**, a clutch wear reduction of **37%**, and a jerk reduction of **60%** in the inertia phase. These results are good compared to the results of the methods surveyed in Section 4.2.

Chapter 6

Further Work

A lot can be done to improve the model in different senses. The data of some of the look-up tables and some of the variables used has to be verified and probably updated. A more extensive model verification is underway. A more detailed model of the transmission actuator hydraulics, might bring some more valuable information to the upshift dynamics.

The controller is so far only tuned for a single load case. A set of reference signals and controller parameters has to be determined for a number of cases and implemented in a look-up-table-style manner. The TCU then has to choose the most appropriate strategy for each upshift situation.

Furthermore, the controller strategy should be discretized and implemented in the real vehicle for evaluation. If the results seem promising, the transmission model should be expanded to include other gear shifts as well.

The structure of the vehicle model facilitates other control strategies to be tried out, and the model is now also being used for that purpose.

References

- [1] ABB Automation Products AB. ABB Short Presentation. Powerpoint.
- [2] ABB Automation Products AB. Torductor-S Design Guidelines, November 2001.
- [3] J. P. Absmeier. Automatic Transmission Modeling and Controller Development. Master's thesis, Mechanical Engineering, Graduate Division, University of California, Berkeley, California, U.S.A., 2001.
- [4] H. Acker and M. Weber. Meßprinzipien für die Drehmomentmessung zur Antriebsregelung. Technischer Bericht 0002-01, Forschung und Technologie, FT2/EA, DaimlerChrysler, Germany, 2000.
- [5] BOSCH. *Kraftfahrtechnisches Taschenbuch*. Robert Bosch GmbH, Stuttgart, Germany, March 2002.
- [6] J. C. Gerdes C. R. Carlson. Nonlinear Estimation of Longitudinal Tire Slip Under Several Driving Conditions. Paper, Stanford University, Mechanical Engineering, Stanford, CA 94305-4021, USA.
- [7] D. Cho and J. K. Hedrick. Automotive Powertrain Modeling for Control. *Journal of Dynamic Systems, Measurement, and Control*, 111:568–576, December 1989.
- [8] Methode Electronics. Chrysler REE / WRE Transmission Magnetoelastic Torque Sensor. Presentation Material, October 1998. This presentation highlights the magnetoelastic technology and significant events related to the joint Methode / Chrysler project on the REE transmission.
- [9] B. Martin et al. Chrysler 45RFE: A New Generation Real-Time Electronic Control RWD Automatic Transmission. Technical Report 1999-01-0755, SAE, 1999.
- [10] C. Wallin et al. Engine Monitoring of a Formula 1 Racing Car based on Direct Torque Measurement. Technical Report 02P-195, SAE, 2002.

-
- [11] D. Assanis et al. Validation and Use of SIMULINK Integrated, High Fidelity, Engine-In-Vehicle Simulation of the International Class VI Truck. Technical Report 2000-01-0288, SAE, 2000.
- [12] I. J. Garshelis et al. Development of a Magnetoelastic Torque Transducer for Automotive Transmission Applications. Technical Report 970605, SAE, 1997.
- [13] K. J. Yang et al. A Robust Control for Engine and Transmission Systems: Enhancement of Shift Quality. *JSME International Journal*, 44(3):697–707, 2001.
- [14] K. Kurat et al. A Study of Smooth Gear Shift Control System with Torque Feedback. Paper, Hitachi, Ltd., 2520 Takaba, Hitachinaka-shi, Ibaraki-ken, 312 Japan.
- [15] A. Haj-Fraj and F. Pfeiffer. A model based approach for the optimization of gearshifting in automatic transmissions. *Int. J. of Vehicle Design*, 28(1/2/3):171–188, 2002.
- [16] J. B. Heywood. *Internal Combustion Engine Fundamentals*, chapter 9. McGraw-Hill, April 1988.
- [17] J. Koch. *Modellbildung und Simulation eines Automatikgetriebes zur Optimierung des dynamischen Schaltungsablaufs*. PhD thesis, Fakultät Physik, Universität Stuttgart, Stuttgart, Germany, August 2001.
- [18] The MathWorks, Inc., Cochituate Place, Natick, MA. U.S.A. *Matlab: Technical reference*, 6 edition, 2000.
- [19] H. B. Pacejka. *Tyre and Vehicle Dynamics*. Butterworth-Heinemann, December 2002.
- [20] M. Pettersson. *Driveline Modeling and Control*. Phd thesis 484, Department of Electrical Engineering, Linköpings Universitet, Linköping, Sweden, April 1997.
- [21] A. M. Schmid. *Optimale Regelung für Systeme mit variabler Struktur*. PhD thesis, Eidgenössischen Technischen Hochschule Zürich, Zurich, Switzerland, 1994.
- [22] J. S. Souder. Powertrain Modeling and Nonlinear Fuel Control. Master's thesis, Mechanical Engineering, Graduate Division, University of California, Berkeley, California, U.S.A., 2002.
- [23] C. Wallin and L. Gustavsson. Non-Contact Magnetostrictive Torque Sensor—Opportunities and Realisation. Technical report, ABB Automation Technology Products AB, Västerås, Sweden, March 2002. Presented at VDI/VDE-IT 6th International Conference—Advanced Microsystems for Automotive Applications, Berlin, Germany.

Notation

Variables and Parameters

a	Vehicle Acceleration
AR_2	Clutch Number Two Area
β	Road Grade
c	Drive Shaft Damping
C	Vehicle Jerk
c_{2slip}	Differential Speed of Clutch Number Two
δ	Engine Controller Input Bias
e_{engine}	Input to Engine Controller
$e_{pressure}$	Input to Pressure Controller
η	Efficiency of Drive Shaft
f_c	Torque Converter Capacity Factor Look-up Table
f_t	Torque Converter Torque Ratio Look-up Table
F_{drag}	Drag Force Acting on the Vehicle
F_s	Slip Force
F_w	Wheel Force
g	Gravitational Constant
i_1	First Gear Gear Ratio
i_2	Second Gear Gear Ratio
i_{diff}	Differential Gear Ratio
I_{ci}	Input Carrier Gear Inertia
I_{ci12}	Input Carrier Inertia during 1-2 Gear Upshift
I_{cr}	Reaction Carrier Gear Inertia
I_{cr12}	Reaction Carrier Inertia during 1-2 Gear Upshift
I_{ds}	Drive Shaft Inertia
I_e	Engine Inertia
I_g	Lumped Gear Box Inertia
I_p	Pump Inertia
I_{si}	Input Sun Gear Inertia

I_{si12}	Input Sun Inertia during 1-2 Gear Upshift
I_t	Turbine Inertia
I_{t1}	Turbine Equivalent Inertia in First Gear
I_{t2}	Turbine Equivalent Inertia in Second Gear
I_w	Wheel Inertia
m	Vehicle Mass
μ	Road-Tire Friction Constant
μ_1	Clutch Number Two Static Friction Constant
μ_2	Clutch Number Two Dynamic Friction Constant
μ_{c2}	Clutch Number Two Friction
k	Drive Shaft Stiffness
$\Delta\dot{\phi}$	Differential Speed
P_0	Predefined Pressure Profile Maximum Pressure
$P_{actual:c2}$	Pressure Exerted on Clutch Two
P_{c2}	Clutch Number Two Predefined Pressure Profile
$P_{commanded:c2}$	Pressure Commanded on Clutch Two
Q	Dissipated Energy
r_w	Wheel Radius
s	Wheel Slip
τ	Pressure Dynamics Time Constant
$\dot{\theta}_{ci}$	Input Carrier Speed
$\dot{\theta}_{cr}$	Reaction Carrier Speed
$\dot{\theta}_{ds}$	Drive Shaft Speed
$\dot{\theta}_e$	Engine Speed
$\dot{\theta}_g$	Gearbox Output Speed
$\dot{\theta}_p$	Pump Speed
$\dot{\theta}_{si}$	Input Sun Speed
$\dot{\theta}_{sr}$	Reaction Sun Speed
$\dot{\theta}_t$	Turbine Speed
$\dot{\theta}_w$	Wheel Speed
T_{break}	Break Torque Applied on Wheels
T_{c2}	Clutch Number Two Reaction Torque
T_d	Differential Reaction Torque
$T_{des:ds}$	Transmission Output Desired Torque
T_{ds}	Drive Shaft Torque
T_e	Engine Torque
$T_{fr:e}$	Engine Internal Friction Torque
$T_{fr:g}$	Gear Box Internal Friction Torque
$T_{fr:w}$	Wheel Friction Torque
T_g	Gear Box Reaction Torque

T_p	Pump Reaction Torque
$T_{Rc2down}$	Reaction Torque on one side of the Second Clutch
T_{Rc2up}	Reaction Torque on one side of the Second Clutch
T_{Rsp1}	Reaction Torque of First Clutch Sprag
T_t	Turbine Reaction Torque
T_w	Wheel Torque
v	Vehicle Speed

Glossary

In Order of Appearance:

Drive Train

Includes all the moving parts of the vehicle, from the engine to the wheels

Powertrain

The first part of the drivetrain, including the engine and the transmission

Driveline

The driveline includes everything beyond the engine and transmission.

AT

Automatic Transmission

TC

Torque Converter

PGS

Planetary Gear Set

TCU

Transmission Control Unit

TP

Torque Phase

IP

Inertia Phase

SAW

Surface Acoustic Wave

Appendix A

Torque Sensing

In modern cars the torque information is extracted from lock-up tables that can not take individual variances and wear into account. A torque sensor would be a straight forward solution to the problem of not knowing the exact torque. Today there is a smorgasbord of sensors available to choose from, ranging from the sensors based on the more primitive strain gauge principle to the non-contact magnetoelastic¹ principle. The sensor principles are surveyed after the following discussion about the two main torque sensor categories [4, 12]. Those are:

- Angular displacement measurement
- Transducer on the torque transmitting shaft

The angular displacement method is measuring the torsion angle using a setting with sensors and cogwheels in both ends of a shaft. The magnitude of the displacement angle is then translated to calculate the applied torque. Since this kind of torque measurement requires a substantial length of the shaft, it is most likely not applicable for implementation in the power train. There are also other deficits associated with this method when it comes to the sensors at the drive shaft ends. Among them are:

1. An angular displacement sensor using Hall sensors for detection is temperature dependent
2. An optical sensor, e.g. a laser diode, needs to be hermetically encapsulated to avoid contamination
3. The sensor fixation must be made very reliable

The above mentioned reasons are good enough to look at the other type of torque sensing mentioned above. The different sensor principles in this category are discussed in the next section.

¹also called magnetostrictive

A.1 Sensor Principles

The sensor principles most likely to be considered for drive train implementation are [4, 8, 12]:

- Strain gauges: Using a strain gauge bridge on the rotating shaft to measure the local strain which in turn is translated to torque. Strain gauges are dependable for measuring stress, but requires electronics to rotate with the shaft. Furthermore, the automotive environment might be too harsh for this construction relying on adhesive bonding of components.
- Surface Acoustic Wave (SAW). This method utilizes transducers mounted on the rotating drive shaft that measure ultrasonic pulse propagation time between same. The propagation time is stress dependent and hence torque dependent. The problem is the transducers have limited strain capacity, they might break. Also, a flat surface is needed to apply the transducer and the application process itself is rather complicated and labor intensive. On the other hand, the resonant frequency is measured and therefore there is no signal noise.
- A sensor based on the capacitive principle has been considered a good candidate for drive train implementation. This type of sensor measures the change in capacity between two radially mounted electrodes from which one is displaced by the applied torque. So far it has been felt as not being rough enough.
- Magnetoelastic: It is well known that stress alters the orientation of the spontaneous magnetization readily present in ferromagnetic materials. This phenomenon facilitates non-contact magnetic determination of the transmitted torque. A number of ways to utilize this have been practiced over the years. One setting considered is using a magnetoelastic ring for transducer pressed axially onto the shaft combined with a non-contact field sensor. It has also been considered to use a shaft simply as its own transducer, comprised of a suitable metal. The latter might be suitable for the sensor application, but might in a sense not provide the desired mechanical characteristics. Some other problems associated with this type of torque sensors are:
 1. The effective permeability of a surface varies significantly with for instance temperature
 2. Permeability is not a single material dependent property, it depends on the characteristics of the measuring field, and hence:
 3. The sensor linearity, hysteresis, dynamic range, and temperature effects are all depending on the excitation field parameters

Another approach is to use a magnetically polarized ring for transducer. This would be one way to get around the permeability dependency

problem. However, one of the main drawbacks is clear, the sensor would attract ferric particles and the long term durability of the polarization have not been proved. Instead, a method that seems to have been neglected till recently, is using eddy currents induced in copper conductors electroplated on the drive shaft [23]. This sensor has shown promising performance characteristics, and among the considered most important are [8]:

- Accuracy
- Repeatability
- Durability
- Hysteresis
- Temperature Coefficient
- Linearity
- Immunity to EMI and RFI

The sensor is comprised of the above mentioned copper pattern and uses two separate coil systems. One is for creating a rotationally symmetric magnetic field in the shaft and the other is for measuring the induced voltages on the copper pattern caused by changes in the magnetic flux, in turn induced by the torsional load. The copper pattern is designed in such a way it aligns with the principle stress direction, see Figure A.1. This contributes to fulfill the desirable characteristics [2, 4, 23], from which some were listed above. It has also proven to meet the demanding requirements of a Formula One race car implementation [10]. This is the kind of sensor DaimlerChrysler decided to use in the project this thesis is part of. The sensor placement and its associated pros and cons are discussed in the rest of this appendix.

A.2 Sensor Location

Depending on where the torque sensor is implemented in the drive train different properties of the drive train dynamics can be monitored, in addition to the torque measurement itself. There are in general two locations that are considered for torque sensor implementation. One is on the engine output shaft and the other is on the transmission output shaft. They are further discussed below.

A.2.1 Between Engine and Transmission

The closer to the engine the sensor is located, the more information about the engine the sensor signal contains. This type of sensor location facilitates

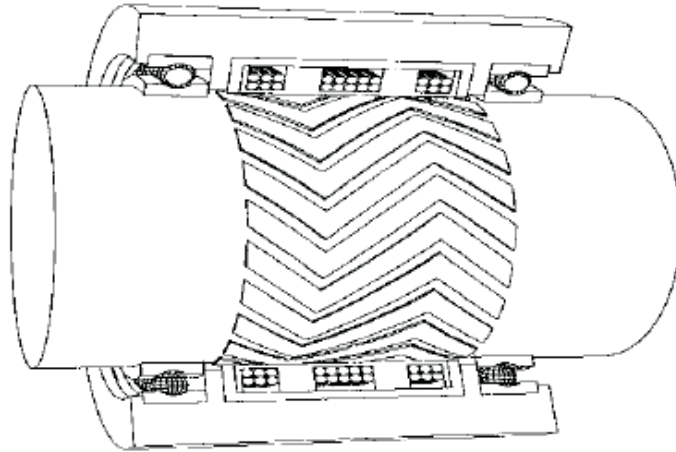


Figure A.1: Schematics of the Magnetoelastic Sensor [23]

accurate verification of engine models and makes it possible to monitor the engine's internal combustion process. That means sensor information can be used for, for example, detecting engine knock and for monitoring engine performance. Other applications the sensor signal can be considered for are [1]:

- Improved Idling Control
- Individual Cylinder Balancing
- Monitoring Engine Deterioration
- Detection of Zero Torque for Clutch and Gear Shift Timing

The accuracy of torque estimated from models and look-up tables is ranging between 65-95 percent [23], and since the torque information is needed by most engine control systems today, the benefit from a true torque value is clear. The deficit in a broader perspective is that shift quality and transmission performance can not be monitored very close using this sensor location.

A.2.2 Behind Transmission

Placing the sensor behind the transmission, i.e. on the gear box output shaft, enables monitoring of the gear box output torque along with the dynamic behavior of same, and that of the drive train. The potential of improving

driveability and shift quality is well known, see for example [8, 10, 12, 17, 20]. A true transmission output torque signal enables a variety of control possibilities, among those are:

- Gear Shift Control and Management
 - Drive line control based on a combination of transmission speed and torque output feedback has already shown promising theoretical gear shift quality improvements [17]
 - The measured torque can be fed back to the transmission control unit optimizing shift scheduling in a fuel saving sense [8]
 - A real world torque signal would help eliminate the influence of vehicle to vehicle variation
- Gear Box and Drive Line Monitoring
 - Gear box deterioration, e.g. on clutches and bands, might be possible to detect and measure
 - Detecting rough road conditions and drive line abuse would be possible

Copyright

Svenska

Detta dokument hålls tillgängligt på Internet - eller dess framtida ersättare - under en längre tid från publiceringsdatum under förutsättning att inga extraordinära omständigheter uppstår.

Tillgång till dokumentet innebär tillstånd för var och en att läsa, ladda ner, skriva ut enstaka kopior för enskilt bruk och att använda det oförändrat för ickekommersiell forskning och för undervisning. Överföring av upphovsrätten vid en senare tidpunkt kan inte upphäva detta tillstånd. All annan användning av dokumentet kräver upphovsmannens medgivande. För att garantera äktheten, säkerheten och tillgängligheten finns det lösningar av teknisk och administrativ art.

Upphovsmannens ideella rätt innefattar rätt att bli nämnd som upphovsman i den omfattning som god sed kräver vid användning av dokumentet på ovan beskrivna sätt samt skydd mot att dokumentet ändras eller presenteras i sådan form eller i sådant sammanhang som är kränkande för upphovsmannens litterära eller konstnärliga anseende eller egenart.

För ytterligare information om Linköping University Electronic Press se förlagets hemsida: <http://www.ep.liu.se/>

English

The publishers will keep this document online on the Internet - or its possible replacement - for a considerable time from the date of publication barring exceptional circumstances.

The online availability of the document implies a permanent permission for anyone to read, to download, to print out single copies for your own use and to use it unchanged for any non-commercial research and educational purpose. Subsequent transfers of copyright cannot revoke this permission. All other uses of the document are conditional on the consent of the copyright owner. The publisher has taken technical and administrative measures to assure authenticity, security and accessibility.

According to intellectual property law the author has the right to be mentioned when his/her work is accessed as described above and to be protected against infringement.

For additional information about the Linköping University Electronic Press and its procedures for publication and for assurance of document integrity, please refer to its WWW home page: <http://www.ep.liu.se/>